ADDENDUM:

CFD analysis of Vor prop project

By Ibrahim Mesinovic

Contents

Objective
CFD SIMULATION APPROACH
Meshing
Calculation
Post processing
Conclusion

Objective

This study presents computational investigation of the flow in axial water turbines using Finite Volume based commercial CFD package namely Fluent. Based on three dimensional numerical flow analysis and fluid-structure interaction, the flow characteristics of water turbines governing equations.

Mainly the existing generated forces and moments on blades because of the interaction between water and the solid of blades.

CFD SIMULATION APPROACH

CFD is fundamentally based on the governing equations of fluid dynamics. They represent mathematical statements of the conservation laws of physics, where the following physical laws are adopted:

1. Mass is conserved for the incompressible fluid at steady state as

$$\frac{\partial u}{\partial x}+\frac{\partial v}{\partial y}+\frac{\partial w}{\partial z}=0$$

where, the fluid velocity at any point in the flow field is described by the local velocity components and which are functions of location (x,y,z) and time (t).This equation is precisely the partial differential form of the continuity equation.

2. Newton's second law: the rate of change of momentum equals the sum of forces acting on the fluid

Where pressure gradient, and other corresponding terms in these three equations and the normal and tangential stresses acting the control volume body forces that may gravity, centrifugal, Coriolis, and electromagnetic forces.

3. Standard κ-ε mode

Assumptions

In this study, the preprocess including model and non-structure mesh generation was completed.

Since the working fluid is ocean water, the CFD simulations were calculated based on assumptions as follows:

1. Incompressible flow.
2. Steady-state conditions.

3. Thermal effects are negligible.
4. Smooth walls with no-slip boundary condition.

$$\rho\left(u\frac{\partial u}{\partial x}+v\frac{\partial u}{\partial y}+w\frac{\partial u}{\partial z}\right)=-\frac{\partial p}{\partial x}+\frac{\partial \tau_{xx}}{\partial x}+\frac{\partial \tau_{yx}}{\partial y}+\frac{\partial \tau_{zx}}{\partial z}+F_x$$

$$\rho\left(u\frac{\partial v}{\partial x}+v\frac{\partial v}{\partial y}+w\frac{\partial v}{\partial z}\right)=-\frac{\partial p}{\partial y}+\frac{\partial \tau_{xy}}{\partial x}+\frac{\partial \tau_{yy}}{\partial y}+\frac{\partial \tau_{zy}}{\partial z}+F_y \quad (3$$

$$\rho\left(u\frac{\partial w}{\partial x}+v\frac{\partial w}{\partial y}+w\frac{\partial w}{\partial z}\right)=-\frac{\partial p}{\partial x}+\frac{\partial \tau_{xz}}{\partial x}+\frac{\partial \tau_{yz}}{\partial y}+\frac{\partial \tau_{zz}}{\partial z}+F_z$$

$$\frac{\partial}{\partial t}(\rho k)+\frac{\partial}{\partial t}(\rho k u_i)=\frac{\partial}{\partial x_j}\left[\left(\mu+\frac{\mu_t}{\sigma_k}\right)\frac{\partial k}{\partial x_j}\right]+G_k-\rho\varepsilon$$

$$\frac{\partial}{\partial t}(\rho\varepsilon)+\frac{\partial}{\partial x_i}(\rho\varepsilon c)=\frac{\partial}{\partial x_j}\left[\left(\mu+\frac{\mu_t}{\sigma_\varepsilon}\right)\frac{\partial \varepsilon}{\partial x_j}\right]+C_1\frac{\varepsilon}{k}G_k-C_2\rho\frac{\varepsilon^2}{k}$$

Calculation

Calculation Solver:

3D Segregated Steady Implicit Solver Turbulence Model: Standard k–ε model, standard wall functions. Multiple Reference Frames (MRF) approach was used to modeling the rotating flow. This approach adopts two reference frames; one stationary frame related to the body walls around impeller; the other related to the rotating impeller. The fluid zone is

divided into two separate regions, while the other, close to the rotating impeller, is related to the moving zone. The momentum equations and closure models are resolved in the separate zones and a steady state approximation is made at the zone interface. Reliable results can be given only by a well converged, well posed and grid independent simulation. Convergence is determined by the order of magnitude of the residues. Two different convergence tolerances are calculated, one is 10^{-4}, and the other is 10^{-6} for continuity of flow in this study. Running the solver such that residuals fall one more order of magnitude means that more iteration is done to improve the solution quality. It should be noted that convergence criteria must assure that the results do not change as the iterations proceed. In this study the mass flow rate change was monitored

When the mass flow rate stays at a certain number and does not change as the iterations continue, then it can be stated that solution has converged. It was seen that this criterion was satisfied when the continuity and momentum residues fell below 10^{-6}.

Meshing

The mesh, or grid, is the discretized domain in which the flow problem is to be solved. The flow properties are calculated in each cell, and hence, as briefly described, the density of the cells (i.e. the mesh resolution) is of great importance. Basically, the grid could be either structured or unstructured. In an unstructured grid, the cells are arranged in an apparently random fashion in contrast to a structured grid.

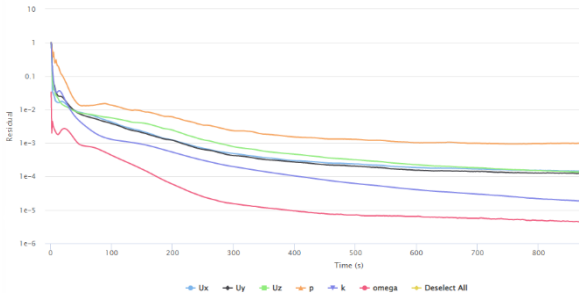
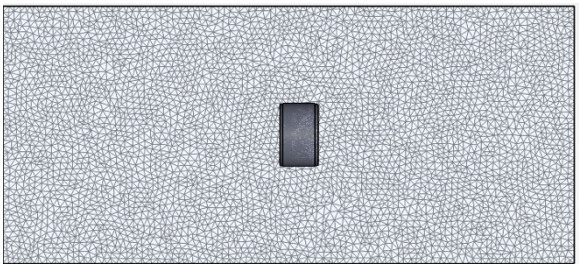


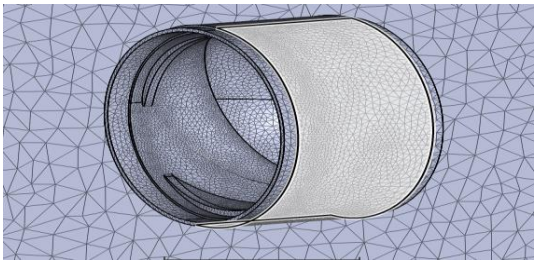
Figure Convergence tolerance 10-4

Further, the mesh could be either single- block or multi-block. For instance, in a structured single-block mesh, the gridlines must pass through the entire domain. For complex geometries, multi-block grids are necessity as it is in our case.

The final judgment on the quality of the division is made through several points, the most important of which is the overall mesh quality which ranges from 0.035 to 1.0
As it is shown in the next figure.

Overall mesh quality:	0.107 (Acceptable range: 0.035 to 1.0)
This mesh meets our quality criteria.	





The way of meshing in our case it divide the domain to two main sources ,the first one is computational domain and the second which is needed to be specific in number of elements ,shape and quality in the region which the flow will be influenced by the structure as the casing and the blades of the turbine .So, the sizing of elements has become more smaller and more numerous in the region of blades with more inflation considerations around the layer where the fluid structure interaction happens .

Mesh densities in the regions: single turbine unit and free flow. Mesh inflation around the blade and the casing. In our case, different types of elements have been used: prims, tetrahadedra, quadrangles,.....,etc

As it is shown in the next table the used type of element and its number:

Number of nodes:	331962
Number of edges:	4153
Number of faces:	2487322
Number of volumes:	1134452
Number of triangles:	2058503
Number of quadrangles:	428819
Number of tetrahedra:	877050
Number of hexahedra:	60692
Number of prisms:	148388
Number of pyramids:	48322

Post processing

Path line plots:

Path lines are parallel to the mean velocity vector, where they trace the flow pattern using massless particles.

Vector plots: A vector plot provides the means whereby a vector quantity is displayed at discrete points (usually velocity, with arrows) whose orientation indicates direction and whose size indicates magnitude.

To calculate the extracted power, the first law of thermodynamics was used, which indicates that the rate of change of energy equals the sum of rate of heat addition on and the rate of work done on the fluid.

Where, **Q** is the heat transfer, **W** is the work being done, h is the specific enthalpy, **0.5 C^2** is the kinetic energy per unit mass and **gz** is the potential energy per unit mass. For an incompressible fluid (liquid water), in the absence of friction, the maximum work output from the turbine is

$$Q - W = m\left[(h_2 - h_1) + \frac{1}{2}(c_2^2 - c_1^2) + g(z_2 - z_1)\right] \quad \frac{1}{2}c^2$$

$$\dot{W} = \dot{m} g [H_1 - H_2]$$

$$\text{where, } gH = \frac{p}{\rho} + \frac{1}{2}c^2 + gz$$

For a control volume and steady state, the law of moment of momentum can be obtained.

which states that, the sum of the moments of the external forces acting on fluid temporarily occupying the control volume is equal to the net time rate of efflux of angular momentum from the control volume

$$\tau = \dot{m}(r_1 C_{u1} - r_2 C_{u2})$$

From Euler's equation the turbine extract power is given as follows:

$$\dot{W} = \tau\omega = \omega\dot{m}(r_1 C_{u1} - r_2 C_{u2})$$

In axial turbine $r_1 = r_2$.

The extract power of 1.02 kw at a nozzle inlet speed of 1.8m/s for a first model with a 0.2m diameter wound turbine is very encouraging.

The following figure shows the forces existing on the blades.

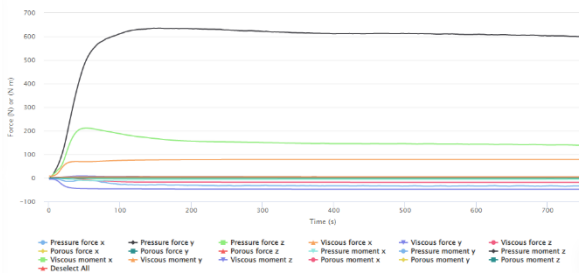


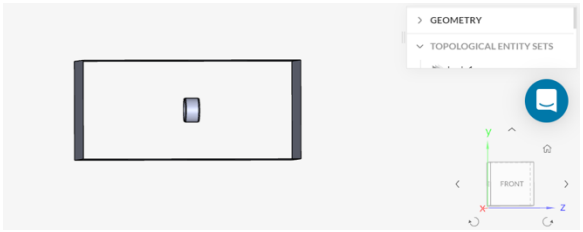
Figure 1 forces and moments of blade

Type value	unit
Pressure force X 32.5	N
Pressure force y 587.6	N
Pressure force Z 133.8	N
Viscous force X 78.6	N
Viscous force Y 5.6	N
Viscous force Z 18.3	N
Viscous moment X 1.2	N.m
Viscous moment Y 4.7	N.m
Viscous moment Z 47.4	N.m
pressure moment X 5.3	N.m
pressure moment Y 0.025	N.m
pressure moment Z 5.1	N.m

Turbine axis

The orientation of the blade as it exists in the computational domain the Z direction is the axial direction of the blade and both of x,y directions are the radial direction of flow.

As it is shown in the next figure



Turbine characteristics

Rotating speed (rpm).	1500
Mass flow rate (kg/s)	18.5
Tangential velocity:(cu)m/s	1.8
Power (kw)out.	1.0205
Torque in x direction N.m	6.66

Results

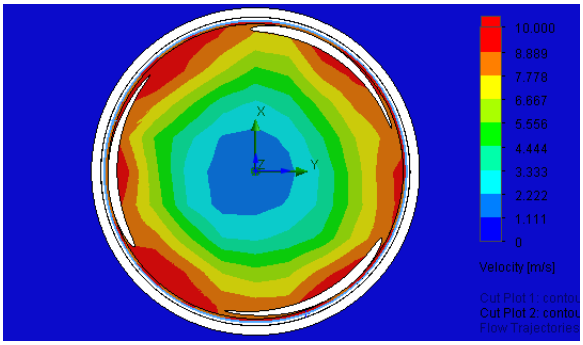


Figure Velocity contour diagram of single turbine unit placed in free flow of 8 m/s

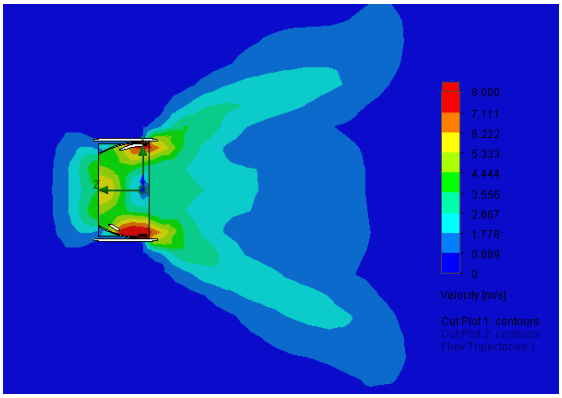


Figure Velocity contour diagram of single turbine unit normal view

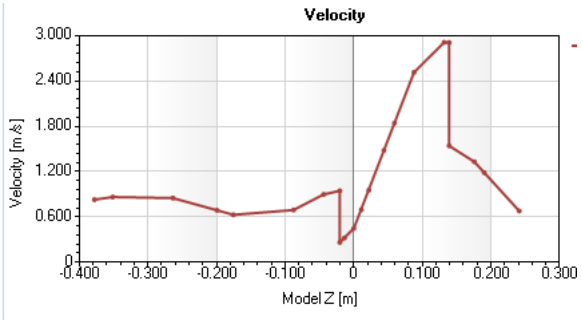


Figure axial velocity across the turbine

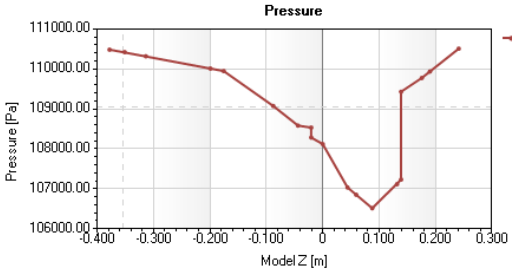


Figure axial pressure difference across the turbine

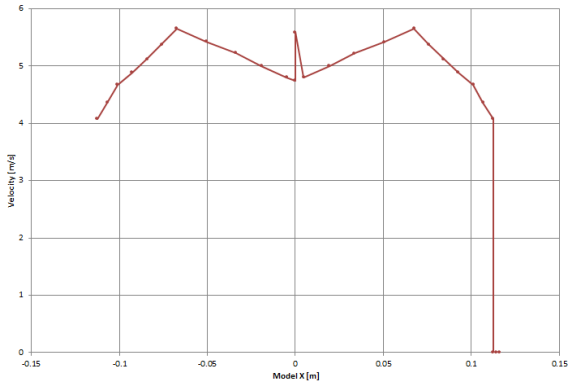


Figure Radial velocity distribution at the inlet of turbine

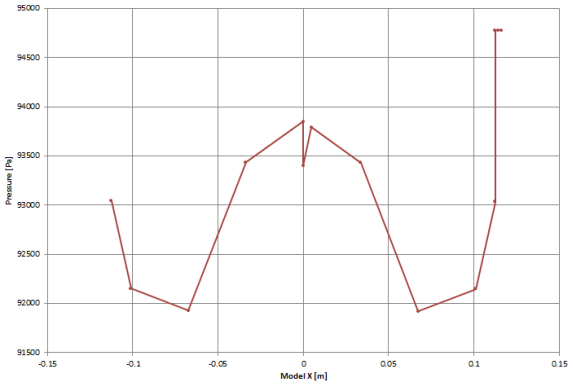


Figure Radial pressure difference at the inlet of turbine

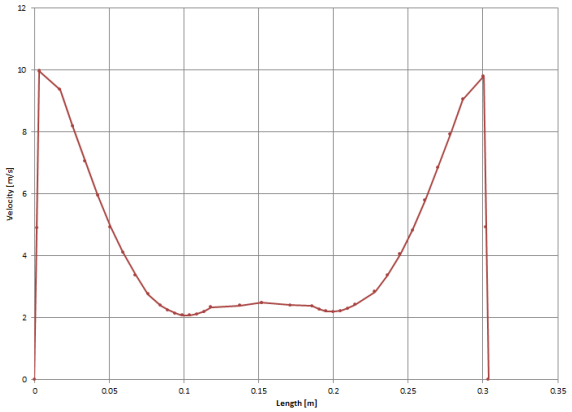


Figure Radial velocity distribution at the outlet of turbine

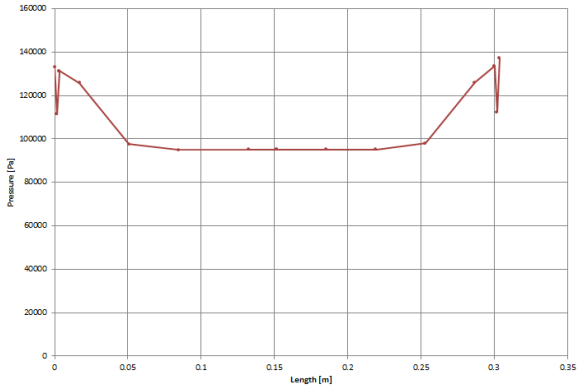


Figure Radial pressure difference at the outlet of turbine

From the previous results, it is possible to determine what is the possible improvement of the distribution of speeds at the inlet and outlet of the turbine, as well as the pressure difference at the inlet and outlet of the turbine.

It is also important to anticipate water movement after getting out from turbine there are some areas where water circulation occurs.

It is important to reduce those areas as these areas reduce the tangent velocity of water after turbine, which affect badly the extract torque and power of the turbine.

So, the next action is: How can you reduce those eddies that occurred in the water.

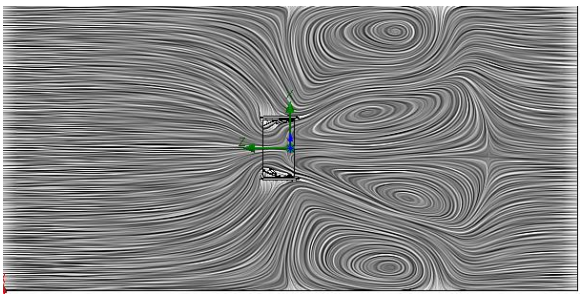


Figure streamlines of water show the areas of circulations of water

Conclusion

The mesh which was used, multi block grid unstructured types like were mentioned ***prims, tetrahadedra, quadrangles*** and the number of meshing is about 4.5 million as they were mentioned. The overall quality of meshing is acceptable as previous mentioned.

The analysis was done with some assumptions as they were previously described. The residuals of solution were about 10^-4 which is considered acceptable.

The results as were discussed, the difference in the tangential velocity between exit and inlet is about 1.8 m/s, generated water with flow rate about 18.5 kg/s and the efficiency of the turbine is about 0.68 as there some obvious losses in circulation of water after water passing away the turbine which decreases the tangential velocity of the turbine.

video introduction:
https://youtu.be/1nDOpNKP1-E

Thank you for your interest and recommendations.

Richard P. Hayman, Director

Vor-Prop LLC
290 Quaker Rd.
Pomona NY 10970 USA

riphear@aol.com
1-914-263-6716